HHS Public Access

Author manuscript

Angew Chem Int Ed Engl. Author manuscript; available in PMC 2022 March 26.

Published in final edited form as:

Angew Chem Int Ed Engl. 2020 December 21; 59(52): 23772–23781. doi:10.1002/anie.202011171.

Exploiting the Potential of Meroterpenoid Cyclases to Expand the Chemical Space of Fungal Meroterpenoids

Takaaki Mitsuhashi[+],
Graduate School of Pharmaceutical Sciences, The University of Tokyo 7-3-1 Hongo, Bunkyo-ku, Tokyo 113-0033 (Japan)

Division of Advanced Molecular Science, Institute for Molecular Science, National Institutes of Natural Sciences 5-1 Higashiyama, Myodaiji, Okazaki, 444-8787 (Japan)

Lena Barra[+],
Graduate School of Pharmaceutical Sciences, The University of Tokyo 7-3-1 Hongo, Bunkyo-ku, Tokyo 113-0033 (Japan)

Zachary Powers[+],
Department of Chemistry and Center for Molecular Discovery (BU-CMD), Boston University, Boston, Massachusetts, 02215 (USA)

Volga Kojasoy[+],
Department of Chemistry, University of California Davis 1 Shields Avenue, Davis, California 95616 (USA)

Andrea Cheng,
Department of Chemistry and Center for Molecular Discovery (BU-CMD), Boston University, Boston, Massachusetts, 02215 (USA)

Feng Yang,
Department of Chemistry and Center for Molecular Discovery (BU-CMD), Boston University, Boston, Massachusetts, 02215 (USA)

Yoshimasa Taniguchi,
Central Laboratories for Key Technologies, Kirin Holdings Co. Ltd. 1-13-5, Fukuura Kana-zawa-ku, Yokohama-shi, Kanagawa, 236-0004 (Japan)

Takashi Kikuchi,
Rigaku Corporation, 3-9-12 Matsubara-cho, Akishima-shi, Tokyo 196-8666 (Japan)

Makoto Fujita,
Division of Advanced Molecular Science, Institute for Molecular Science, National Institutes of Natural Sciences 5-1 Higashiyama, Myodaiji, Okazaki, 444-8787 (Japan)

[*] abei@mol.f.u-tokyo.ac.jp, porco@bu.edu, djtantillo@ucdavis.edu.
[+]These authors contributed equally to this work.

Supporting information and the ORCID identification number(s) for the author(s) of this article can be found under: https://doi.org/10.1002/anie.202011171.

Conflict of interest The authors declare no conflict of interest.

Department of Applied Chemistry, Graduate School of Engineering, The University of Tokyo, 7-3-1 Hongo, Bunkyo-ku, Tokyo 113-8656 (Japan)

Dean J. Tantillo*,
Department of Chemistry, University of California Davis 1 Shields Avenue, Davis, California 95616 (USA)

John A. Porco Jr*,
Department of Chemistry and Center for Molecular Discovery (BU-CMD), Boston University, Boston, Massachusetts, 02215 (USA)

Ikuro Abe*
Graduate School of Pharmaceutical Sciences, The University of Tokyo 7-3-1 Hongo, Bunkyo-ku, Tokyo 113-0033 (Japan)

Collaborative Research Institute for Innovative Microbiology, The University of Tokyo, Yayoi 1-1-1, Bunkyo-ku, Tokyo 113-8657 (Japan)

Abstract

Fungal meroterpenoids are a diverse group of hybrid natural products with impressive structural complexity and high potential as drug candidates. In this work, we evaluate the promiscuity of the early structure diversity-generating step in fungal meroterpenoid biosynthetic pathways: the multibond-forming polyene cyclizations catalyzed by the yet poorly understood family of fungal meroterpenoid cyclases. In total, 12 unnatural meroterpenoids were accessed chemoenzymatically using synthetic substrates. Their complex structures were determined by 2D NMR studies as well as crystalline-sponge-based X-ray diffraction analyses. The results obtained revealed a high degree of enzyme promiscuity and experimental results which together with quantum chemical calculations provided a deeper insight into the catalytic activity of this new family of non-canonical, terpene cyclases. The knowledge obtained paves the way to design and engineer artificial pathways towards second generation meroterpenoids with valuable bioactivities based on combinatorial biosynthetic strategies.

Keywords

chemoenzymatic synthesis; combinatorial biosynthesis; crystalline-sponge *x*-ray diffraction; meroterpenoid cyclase; meroterpenoids

Introduction

Fungal meroterpenoids have earned significant interest from the scientific community as well as from the pharmaceutical and chemical industry due to their remarkable structural architectures and potent bioactivities.[1] Pyripyropene A (**1**), isolated from *Aspergillus fumigatus*, is the strongest known inhibitor of acyl-CoA:cholesterol acyltransferase and is being developed for the treatment of atherosclerosis.[2] Additionally, **1** exhibits insecticidal properties and a commercial insecticide based on the pyripyropene core structure has been recently marketed.[3] Derivatives of mycophenolic acid (**2**), isolated from *Penicillium* sp., are clinically used immunosuppressant drugs and inhibit inosine 5′-monophosphate

dehydrogenase.[4] Andrastin A (**3**) from *Penicillium albocoremium* is an inhibitor of protein farnesyl transferase and a potent anti-cancer agent,[5] whereas tropolactone D (**4**) from *Aspergillus* sp. is a cytotoxic agent against human colon carcinoma (Figure 1A).[6] The genetic basis for fungal meroterpenoid biosynthesis has only been elucidated in recent years, with the first biosynthetic gene cluster reported for pyripyropene A in 2010.[7]

Since then, the discovery of several related gene clusters revealed a common modular assembly logic for all meroterpenoid pathways, composed of i) building block generation (polyketide synthase, oligoprenyl synthase), ii) assembly of building blocks (prenyltransferase), iii) early structural diversification by an epoxidase enzyme followed by action of a novel family of terpene cyclases and iv) late stage diversification by tailoring enzymes such as cytochrome P450 monooxygenases and α-ketoglutarate-dependent dioxygenases.[8] Their strong biological activities as well as the conserved modular logic of their biosynthetic pathways make meroterpenoids attractive targets for artificial pathway engineering to generate novel structures with new and improved activities. Herein, we set out to evaluate the potential of meroterpenoid cyclases to generate novel scaffolds by employing natural and unnatural synthetic substrate analogues. The results obtained provide valuable information on matching pathway combinations regarding the interchange-ability of employed meroterpenoid cyclases. At the same time, chemoenzymatic access to eight new scaffolds, thus far unprecedented from natural sources or chemical, biomimetic polyene cyclizations, could be achieved.

Results and Discussion

Targeted Enzymes and Synthesis of Substrates

Non-canonical terpene cyclases involved in meroterpenoid biosynthesis are integral membrane proteins of compact size (ca. 25 kDa).[7,8] Mutagenesis studies on the model cyclase Pyr4 involved in the pyripyropene biogenesis revealed two highly conserved acidic amino acid residues (Glu63 and Asp218) crucial for enzyme function which are proposed to initiate polyene cyclization by protonation of the terminal epoxide function of the substrate thereby triggering subsequent polyene cyclization (Figure 1B). The mechanism resembles that of type-II terpene synthases of the 2,3-oxidosqualene-lanosterol cyclase type; however, protein structural data to evaluate the mechanism of meroterpenoid cyclases is still lacking.[7–9] Phylogenetic analysis of characterized meroterpenoid cyclases shows a close relation to the group of Pyr4-like synthases involved in fungal indole diterpene biosynthesis (LtmB, AtmB, and PaxB) and a distant relation to the bacterial enzymes XiaE and DmtA1 (Figure 2).[10] The protein sequence alignment for selected enzymes is shown in Figure S6A.

The substrates of known meroterpenoid cyclases are composed of a linear epoxyoligoprenyl chain, in most cases derived from farnesyl diphosphate (FPP) and a distinct non-terpenoid portion usually generated by a designated polyketide synthase (Figure 2). These biosynthetic intermediates are difficult to obtain from enzymatic reactions, since typically low concentrations are observed and the frequently employed heterologous expression host *Aspergillus oryzae* contains endogenous hydrolases producing high amounts of a shunt diol product.[7] To overcome this limitation, we recently developed a modular synthesis of the widespread 3,5-dimethylorsellinic acid (DMOA)-containing substrate family. The

methodology involves base-mediated, regioselective dearomatization of DMOA with farnesyl electrophiles.[11] We expanded the synthetic scope by employing enantiopure (10R)- and (10S)-epoxyfarnesyl building blocks in this reaction to obtain the naturally occurring substrates (10R)- and (10S)-(2E,6E)-5′-DMOA methyl ester (**7a**, **7b**), as well as (10R)- and (10S)-(2E,6E)-3′-DMOA methyl ester (**8a**, **8b**). Additionally, we also accessed unnatural substrates including the (2Z,6E)-epoxyfarnesyl congeners (10R)- and (10S)-(2Z,6E)-5′-DMOA methyl ester (**9a**, **9b**) and (10R)- and (10S)-(2Z,6E)-3′-DMOA methyl ester (**10a**, **10b**) using the same strategy (Figure S1, Figure 3). As dearomative alkylation of DMOA leads to formation of two inseparable diastereoisomers with respect to 3′ and 5′ dearomatization, the substrates obtained were used as diastereomeric mixtures, with fixed stereochemistry for the epoxide moiety (88–98% *ee*). With these substrates in hand, we targeted nine reported meroterpenoid cyclases: Pyr4,[7] CdmG,[12] AndB,[13] AdrI′,[14] NvfL,[15] PrhH,[16] Trt1,[17] AscF,[18] and MacJ.[19]

As we did not gain access to the MacJ producer strain, we cloned the homologous protein MacJ′ from *Penicillium chrysogenum* MT-12 (96% identity). The intron-free genes were expressed in the heterologous host *Saccharomyces cerevisiae* INVSc1 and cell free extracts were prepared and utilized for *in vitro* reactions with synthetic substrates **7a**/**7b**–**10a**/**10b**. Monitoring of the reactions by HPLC revealed a surprisingly high degree of promiscuity as several new products were detected (Figure S2–S5, Table 1).

Substrate Scope of Pyr4 and MacJ′

Pyr4, a cyclase which naturally utilizes the (10*S*)-configured epoxide **5** (Figure 1B), was found to accept the substrates (10*S*)-(2*E*,6*E*)-5′-DMOA (**7a**), (10*S*)-(2*E*,6*E*)-3′-DMOA (**8a**) as well as (10*S*)-(2*Z*,6*E*)-3′-DMOA (**10a**) based on the detection of newly formed peaks in the HPLC chromatogram (Table 1, Figure S2–S5). To elucidate the structures of the putative new enzyme products, we carried out preparative scale transformations in which case reaction of Pyr4 with substrate **7a** led to the isolation of compounds **11** and **12** (Scheme 1A).

Both products exhibit a chair-chair conformation for the A/B ring system, as is also found for the natural cyclization to form pyripyropene E (**6**). However, the terminating cation-quenching step differs for both products, leading to **11** after C–O bond formation and **12** after C–C bond formation. These products were also recently identified from chemical cyclization of *rac*-**7** by using $EtAlCl_2$/Et_2AlCl as Lewis acid promoter.[11] The [3.3.1] bridged structure in **12** is also found in asperterpenes A and B, recently isolated and potent BACE1 inhibitors from *Aspergillus terreus*.[20] As can be delineated from the configuration of position 5′, Pyr4 is able to accept both diastereomers, (10*S*,5′*S*)-**7a** and (10*S*,5′*R*)-**7a**, to form **11** and **12**, respectively. The findings suggest that Pyr4, which usually accepts the bulkier substrate **5**, exhibits some degree of promiscuity towards changes in the polyketide portion. This is further demonstrated by the successful conversion of (10*S*,3′*R*)-**8a** to **13**, as well as (10*S*,3′*S*)-**8a** to **14**. Substrate **8a** carries the epoxyfarnesyl chain connected to the 3′-position of the DMOA-building block instead of the 5′-position as found in **7a**. Products **13** and **14** are also accessed from chair-chair substrate conformations, as observed for the natural reaction of Pyr4 towards the chair-chair product **6**. These findings indicate

that the enzyme active site cavity provides a template for precise arrangement of substrate conformation and guidance of a stereochemically distinct polyene cyclization (Scheme 1B). Their structures were determined by 1D and 2D NMR analyses, and further confirmed by the recently developed crystalline sponge (CS) method which enables “crystallization-free” X-ray crystallography. The method makes use of crystalline porous metal complexes that can absorb and orient a compound of interest. The neat alignment of compounds in the pores of the complex makes them observable by conventional X-ray structure analysis without the need for prior crystallization.[21]

We were also interested in the flexibility of Pyr4 towards changes in the farnesyl chain and therefore subjected substrate analogues **9a**/**9b** and **10a**/**10b** to Pyr4. Indeed, Pyr4 was able to convert (10*S*,3′*R*)-**10a** to the new meroterpenoid **15** bearing a *cis*-fused B/C ring system, presumably derived from a chair-chair substrate conformation (Scheme 1C). The natural substrate of Pyr4 contains an (*S*)-configured epoxide functionality. Interestingly, all productive enzyme substrate combinations were restricted to the (10*S*)-series of substrates, as none of the analogous (10*R*)-epoxy substrates (10*R*)-**7b**, (10*R*)-**8b**, (10*R*)-**9b** or (10*R*)-**10b** were accepted. This finding indicates a strict recognition of the epoxide within the substrate binding site of the enzyme. In addition, we found that MacJ′ can also produce products **13** and **14** from (10*S*)-**8a** and **15** from (10*S*,3′*R*)-**10a** (Scheme 1B/C). MacJ, naturally involved in the biosynthesis of the drimane meroterpenoid macrophorin A, is one of two known Pyr4-like cyclases which do not require substrate activation by epoxidation. Instead, MacJ is able to directly protonate the terminal double bond to initiate cyclization (Figure 2, Figure S6B). It is therefore interesting to note that MacJ′ also exhibits a clear preference for the (10*S*)-stereoisomers of epoxide substrates evaluated (Table 1, Figure S2–5).

Substrate Scope of CdmG and AscF

A meroterpenoid cyclase which is phylogenetically closely related to Pyr4 is CdmG (Figure 2), utilized in the biosynthetic pathway towards chrodrimanins from *Penicillium verruculosum*.[12] Chrodrimanins exhibit strong inhibitory activities against protein tyrosine phosphatase 1B (PTP1B) and are potential drug candidates for the treatment of type 2 diabetes and obesity.[22] CdmG naturally catalyzes the formation of 3-hydroxypentacecilide A (**17**) from (*S*)-configured epoxide **16**. In contrast to Pyr4, CdmG controls the substrate conformation in a chair-boat manner, leading to an inverted stereochemical outcome for the *trans*-configured B/C ring system (Scheme 2A). With this apparent change in conformational control, we were interested in determining the substrate promiscuity of CdmG and the putative differences in product formation.

When CdmG was incubated with synthetic substrates, a high degree of promiscuity was also observed as **7a**, **8a**, **9a**, and **10a** were accepted by CdmG and led to the production of new products (Figure S2–S5, Table 1). Whereas products from substrate (10*S*)-**7a** were found to be too unstable for structural characterization, products from substrates **8a**, **9a**, and **10a** were successfully isolated and structurally characterized. Reaction with (2*E*,6*E*)-configured substrate (10*S*)-**8a** led to formation of compound **18** derived from the (10*S*,3′*S*)-**8a** isomer. The structure of **18** was determined by 2D NMR analysis and was further supported by X-

ray-CS-diffraction data. The stereochemical outcome of the cyclization indeed demonstrated a conserved chair-boat conformational control of the substrate by the enzyme (Scheme 2B).

Reaction of CdmG with (10*S*)-**9a** represents the only case where the two products found were derived from one substrate stereoisomer, in this case (10*S*,5′*S*)-**9a**, leading to the isolation of **19** and **20**. Whereas **19** is produced from a C–O bond forming event, product **20** is derived from C–C bond formation.

In both cases, the same *trans-cis* configuration is observed for the A/B/C-ring system (Scheme 2C). Compounds **19** and **20** have also recently been identified from chemical cyclization where it was further shown that **20** can be rearranged to **19** by formic acid treatment.[11] To confirm the enzymatic origin of **19**, **20** was incubated under enzyme reaction conditions (KPP pH 7.4, 16 h, 30°C) but was found to not interconvert to **19**. Reaction of CdmG with (2*Z*,6*E*)-configured substrate **10a** produced the new meroterpenoids **21** and **15**, derived from a chair-boat substrate conformation (major) and a chair-chair substrate conformation (minor), respectively. As observed for the promiscuity of Pyr4, CdmG also had a strict preference for the epoxide stereoconfiguration, as none of the (10*R*)-epoxides were accepted by CdmG.

AscF from the ascochlorin pathway (Figure S6B) was found to also produce **21** and small amounts of **15** from (10*S*)-**10a** as the only accepted substrate (Table 1, Figure S2–S5) and thus represents a meroterpenoid cyclase with very low tolerance towards alternative substrates.

Substrate Scope of AndB

The meroterpenoid cyclase AndB from the anditomin pathway[13] utilizes DMOA-derived substrate **22** with an (*S*)-configured epoxide to produce preandiloid A (**23**) with a chair-boat conformation (Scheme 3). In contrast to the results discussed for CdmG, which also controls the conformation in a chair-boat manner, AndB was found to exhibit a differing selectivity based on the 3′- and 5′-stereocenters and therefore was found to produce different products (Table 1, Figure S2–S5). Specifically, AndB was found to accept (10*S*,3′*R*)-**8a** to produce the novel meroterpenoid **24** (Scheme 3B). Similar to CdmG and Pyr4, the native conformational control of the prenyl chain was conserved, as a chair-boat substrate arrangement was evident leading to **24**. AndB also accepted the (2*Z*,6*E*)-configured substrate (10*S*,5′*R*)-**9a** leading to the isolation of meroterpenoid **25**. The structure elucidation for **25** was challenging as 2D NMR analysis did not clearly reveal the connectivity between the terpenoid and non-terpenoid portions. Additionally, the relative configuration between the A/B and C/D ring systems were difficult to determine due to ambiguous NOESY correlations. However, we were able to fully establish the structure of **25** using crystalline sponge-X-ray analysis which revealed the presence of an unprecedented 6-5-ring system connected to a 5–6 ring system via a single C–C bond (Scheme 3C).

DFT Calculations for the Formation of 25, 20, CC, and 19

The latter finding was surprising, as all reactions in this study lead to the formation of 6-6-ring systems for the A/B rings and also no natural cyclization towards 6-5-ring systems

has been reported thus far. To gain further insight into the cyclization mechanism for the formation of **25** from (10*S*,5′*R*)-**9a** by AndB, we conducted computational studies using density functional theory (DFT) at the B3LYP-D3(BJ)/6-31G(d,p)//B3LYP/6-31G(d,p) and CPCM(H_2O)-B3LYP-D3(BJ)/6-31G(d,p)//B3LYP/6-31G(d,p) levels[23] (see SI for details). The results (Figure 4) revealed that the first intermediate in the reaction cascade (modelled here in the absence of enzyme) is the monocyclic tertiary cation **A**, generated by an endergonic process via transition state **9a-TS. A** is then converted, 010404e, to **25**-H^+ by an exergonic concerted process consisting of formation of the 5-membered B-ring in tandem with nucleophilic attack of the adjacent oxygen functionality via transition state **A-TS**. Inclusion of implicit solvent (CPCM(H_2O), in parentheses; single point calculations on previously optimized geometries in gas phase) led to lower barriers (Figure 4).[24,25] With either a nonpolar (gas phase) or polar (water) surroundings, the barrier for initial cyclization is high for a biological reaction,[26] however, in the absence of enzyme, reactant (10*S*,5′*R*)-**9a**-H^+ relaxes to a non-productive conformation with an internal hydrogen-bond between the alcohol and epoxide; consequently, conformational preorganization by the enzyme should lower the barrier and this could be assisted by specific oriented noncovalent interactions with the transition state structure. An alternative mechanism for formation of the second ring could involve Markovnikov addition to form a 6–6 intermediate, followed by ring-contraction in concert with tetrahydro-furan ring formation. We find, however, that Markovnikov addition leads directly to a “6-6-6-6” product (**C**) that is not experimentally observed. We were able to optimize tertiary carbocation **B** as a minimum and this species can then undergo ring contraction to yield **25**-H^+, but accessing **B** would require escape from the deep energy well associated with **C** and a large conformational change. The enzyme would, however, have to distinguish between **A-TS** and **A′-TS**, again by conformational biasing and/or well-placed noncovalent interactions with the transition state structure.

Mechanisms for formation of **20** (Figure 5) and **CC** (Figure 6) from protonated stereoisomers of **9a** were also subjected to computational analysis. For both reactions, we found highly asynchronous but concerted pathways in which no discrete carbocationic intermediates are formed. Similar concerted polycyclizations have been reported for related systems.[27] Both reactions also are predicted to be essentially barrierless once productive reactant conformations are attained, suggesting that preorganization controls which product is formed by a given enzyme. Conversion of **20**-H^+ to **19**-H^+ is predicted to be an endergonic process (Figure 7; neutral **19** is predicted to be several kcal mol^{-1} lower in energy than neutral **20**, however[11]), but an appropriately positioned base in a restricted enzyme active site could selectively deprotonate **19**-H^+. The barrier for the **20**-H^+ to **19**-H^+ interconversion is also less certain than others described above, since this reaction involves asynchronous bond-breaking, C–C bond rotation, and bond-making that leads to a “loose” transition state for which entropy and the effects of externally-imposed conformational constraints are difficult to estimate.

Substrate Scope of Trt1, AdrI′, PrhH, and NvfL

Another phylogenetic clade is formed by Trt1, AdrI, AdrI′, AusL, and PrhH (Figure 2). These enzymes share the DMOA substrate (10*R*,5′*R*)-**7b**, but differ with regard to their product specificity. Trt1 catalyzes the formation of preterretonin (**27**) via a chair-chair-chair

substrate conformation forming intermediary cation **26**, followed by Wagner–Meer-wein rearrangement and a terminating deprotonation of H_a. AdrI shares the intermediary cation **26** and rearrangement but differs in the terminating deprotonation side (H_b) producing andrastin E (**28**). AusL and PrhH both catalyze the formation of protoaustinoid A (**29**) from **26** after direct deprotonation of H_c (Scheme 4A). NvfL from the novofumigatonin pathway utilizes a highly similar substrate as Trt1, AdrI, AusL, and PrhH, carrying a free carboxylic acid instead of the methyl ester in the DMOA-unit. The free acid is crucial for enzyme function and the protein catalyzes formation of a spiro-center (Figure S6B).

Consistent with the obvious tight recognition of the polyketide portion necessary to achieve these sophisticated and distinct reactions, a comparable low promiscuity for this group of integral membrane-bound enzymes was observed. Whereas PrhH and NvfL did not accept any of the tested unnatural substrates, both Trt1 and AdrI′ accepted (2*Z*,6*E*)-**9b**, with the natural 5′-substitution pattern in the polyketide portion (Table 1, Figure S2–S5).

However, for these cases products were found to be too unstable for structure determination. To our surprise, we found that Trt1 as well as AdrI′ were able to convert (10*S*)-**7a**, the native substrate with inverted stereochemistry with respect to the epoxide functionality. We succeeded in the isolation of the Trt1-mediated product from (10*S*,5′*R*)-**7a** and the structure was determined to be 3-*epi*-preterretonin (**30**). The formation of this product can be envisioned to occur via a boat-chair substrate conformation (Scheme 4B).[28]

Enzyme Kinetics of Trt1

To shed additional light on the substrate promiscuity of meroterpenoid cyclases, we were interested in the comparison of the K_M values of the natural substrate to unnatural substrate analogous. Synthetic (10*R*,5′*R*)-**7b** is the natural substrate of Trt1, which was also found to accept unnatural (10*S*,5′*R*)-**7a**, and (10*R*)-**9b**. Since Trt1 and other meroterpenoid cyclases cannot be purified, the integral membrane bound enzyme was used as a crude enzyme preparation. To ensure comparable reaction conditions, Trt1 was freshly prepared and used for all kinetic assays on the same day. The results revealed an apparent K_M value of 34 μM for the natural substrate **7b**, whereas a 3-fold (95 μM) and 5-fold (144 μM) higher value was found for substrates **7a** and **9b**, respectively. The V_{max} values were determined as 22 $\mu M min^{-1}$, 7 $\mu M min^{-1}$ and 0.5 $\mu M min^{-1}$, for **7b**, **7a** and **9b**, respectively. These findings indicate that the unnatural substrates have a lower affinity for the enzyme, but the values are of the same order of magnitude and thus further demonstrate the promiscuity observed for this enzyme class.

Conclusion

In summary, we have demonstrated chemoenzymatic access to twelve complex, unnatural DMOA-derived meroterpenoids of which eight represent novel compounds by exploiting the surprisingly high promiscuity of fungal meroterpenoid cyclases.

Synthetic 3,5-dimethylorsellinic acid (DMOA)-containing substrates were prepared using dearomative alkylation and evaluated against nine meroterpenoid cyclases. The results demonstrate tight recognition of the epoxide functionality by the cyclase panel, but tolerance

towards the polyketide portion. The conserved cyclization mechanism initiated by epoxide protonation and rigid control of the substrate conformation in the cyclase active site cavity led to the formation of several variations of naturally occurring meroterpenoid scaffolds, as well as generation of a completely new scaffold, although the number of cyclization steps that are concatenated into concerted processes appears to be system-dependent. The challenging structure elucidation and determination of relative and absolute configurations for the obtained enzyme products was solved by combining 2D NMR data analysis with the recently developed method of crystal-line-sponge-X-ray diffraction analysis. This method allowed us to access the crystallographic data of non-crystalline enzyme products such as **25** for unambiguous structure determination and thus represents a powerful technique in combination with second generation natural product discovery.

The knowledge obtained in this study can be used for the design of artificial pathways by recombining biosynthetic genes in a suitable heterologous production host. Whereas productive enzyme combinations with naturally occurring substrates such as **7a** and **7b** provide a straightforward access by reconstituting known pathways towards these substrates and interchanging the introduced meroterpenoid cyclase, access to (2*Z*,6*E*)-configured prenyl substrates require further engineering efforts, for example, by employing a known bacterial (2*Z*,6*E*)-selective FPP synthase from *Mycobacterium*[29] and optimization of downstream enzymes towards substrates like **9a** and **9b**. Furthermore, the new meroterpenoids obtained can be evaluated as substrates for downstream tailoring enzymes such as α-ketoglutarate-dependent dioxygenases. Since several protein crystal structures have been reported in recent years, protein engineering by either rational strategies or directed evolution represents an exciting opportunity to create novel “unnatural” meroterpenoids with valuable biological properties.[30]

Supplementary Material

Refer to Web version on PubMed Central for supplementary material.

Acknowledgements

We thank the National Institutes of Health (R35 GM-118173, J.A.P., Jr.), a Grant-in-Aid for Scientific Research from the Ministry of Education, Culture, Sports, Science and Technology, Japan (JSPS KAKENHI Grant Number JP16H06443 and JP20H00490 to I.A.; JP19H05461 to M.F.), and the MEXT Nanotechnology Platform Program (Molecule and Material Synthesis) promoted at IMS for research funding. We also thank the Deutsche Forschungsgemeinschaft (DFG BA 6870/1-1) for a postdoctoral research fellowship to L.B. Computational work was supported by the National Science Foundation (CHE-1856416 and supercomputing resources from the XSEDE program via CHE-030089).

References

[1]. a)Cornforth JW, Chem. Br 1968, 4, 102–106; [PubMed: 5640876] b)Geris R, Simpson TJ, Nat. Prod. Rep 2009, 26, 1063–1094; [PubMed: 19636450] c)Kaysser L, Bernhardt P, Nam SJ, Loesgen S, Ruby JG, Skewes-Cox P, Jensen PR, Fenical W, Moore BS, J. Am. Chem. Soc 2012, 134, 11988–11991; [PubMed: 22784372] d)Peng X, Qiu M, Nat. Prod. Bioprospect 2018, 8, 137–149. [PubMed: 29722004]

[2]. a)Ōmura S, Tomoda H, Kim YK, Nishida H, J. Antibiot 1993, 46, 1168–1169;b)Tomoda H, Kim YK, Nishida H, Masuma R, Ōmura S, J. Antibiot 1994, 47, 148–153;c)Das A, Davis MA, Tomoda H, Ômura S, Rudel LL, J. Biol. Chem 2008, 283, 10453–10460. [PubMed: 18285335]

[3]. a)Horikoshi R, Goto K, Mitomi M, Oyama K, Sunazuka T, Ōmura S, J. Antibiot 2017, 70, 272–276;b)Dieleman C, Knieriem T, Krapp M, Kierkus PC, Xu W, Benton K, Patent WO 2012/035010 A1, 2012.

[4]. a)Sintchak MD, Fleming MA, Futer O, Raybuck SA, Chambers SP, Caron PR, Murcko MA, Wilson KP, Cell 1996, 85, 921–930; [PubMed: 8681386] b)Clutterbuck PW, Oxford AE, Raistrick H, Smith G, Biochem. J 1932, 26, 1441–1458; [PubMed: 16744963] c)Canonica L, Kroszczynski W, Ranzi BM, Rindone B, Scolastico C, J. Chem. Soc. *D* 1970, 6, 2639–2643;d)Shaw LM, Nowak I, Ther. Drug Monit 1995, 17, 685–689. [PubMed: 8588242]

[5]. a)Ōmura S, Inokoshi J, Uchida R, Shiomi K, Masuma R, Kawakubo T, Tanaka H, Iwai Y, Kosemura S, Yamamura S, J. Antibiot 1996, 49, 414–417;b)Uchida R, Shiomi K, Inokoshi J, Sunazuka T, Tanaka H, Iwai Y, Takayanagi H, Lmura S, J. Antibiot 1996, 49, 418–424.

[6]. Cueto M, MacMillan JB, Jensen PR, Fenical W, Phytochemistry 2006, 67, 1826–1831. [PubMed: 16500687]

[7]. Itoh T, Tokunaga K, Matsuda Y, Fujii I, Abe I, Ebizuka Y, Kushiro T, Nat. Chem 2010, 2, 858–864. [PubMed: 20861902]

[8]. a)Matsuda Y, Abe I, Nat. Prod. Rep 2016, 33, 26–53; [PubMed: 26497360] b)Barra L, Abe I, Nat. Prod. Rep 2020, 37, in press 10.1039/D0NP00056F;c)Matsuda Y, Awakawa T, Mori T, Abe I, Curr. Opin. Chem. Biol 2016, 31, 1–7. [PubMed: 26610189]

[9]. Rudolf JD, Chang CY, Nat. Prod. Rep 2020, 37, 425–463. [PubMed: 31650156]

[10]. a)Young CA, Bryant MK, Christensen MJ, Tapper BA, Bryan GT, Scott B, Mol. Genet. Genomics 2005, 274, 13–29; [PubMed: 15991026] b)Nicholson MJ, Koulman A, Monahan BJ, Pritchard BL, Payne GA, Scott B, Appl. Environ. Microbiol 2009, 75, 7469–7481; [PubMed: 19801473] c)Tagami K, Liu C, Minami A, Noike M, Isaka T, Fueki S, Shichijo Y, Toshima H, Gomi K, Dairi T, Oikawa H, J. Am. Chem. Soc 2013, 135, 1260–1263; [PubMed: 23311903] d)Kato H, Tsunematsu Y, Yamamoto T, Namiki T, Kishimoto S, Noguchi H, Watanabe K, J. Antibiot 2016, 69, 561–566;e)Yao T, Liu J, Liu Z, Li T, Li H, Che Q, Zhu T, Li D, Gu Q, Li W, Nat. Commun 2018, 9, 4091; [PubMed: 30291234] f)Tsukada K, Shinki S, Kaneko A, Murakami K, Irie K, Murai M, Miyoshi H, Dan S, Kawaji K, Hayashi H, Kodama EN, Hori A, Salim E, Kuraishi T, Hirata N, Kanda Y, Asai T, Nat. Commun 2020, 11, 1830; [PubMed: 32286350] g)Li H, Sun Y, Zhang Q, Zhu Y, Li SM, Li A, Zhang C, Org. Lett 2015, 17, 306–309; [PubMed: 25532029] h)Yaegashi J, Romsdahl J, Chiang YM, Wang CCC, Chem. Sci 2015, 6, 6537–6544. [PubMed: 30090271]

[11]. Powers Z, Scharf A, Cheng A, Yang F, Himmelbauer M, Mitsuhashi T, Barra L, Taniguchi Y, Kikuchi T, Fujita M, Abe I, Porco JA, Angew. Chem. Int. Ed 2019, 58, 16141–16146; Angew. Chem. 2019, 131, 16287 – 16292.

[12]. Bai T, Quan Z, Zhai R, Awakawa T, Matsuda Y, Abe I, Org. Lett 2018, 20, 7504–7508. [PubMed: 30417647]

[13]. a)Matsuda Y, Wakimoto T, Mori T, Awakawa T, Abe I, J. Am. Chem. Soc 2014, 136, 15326–15336; [PubMed: 25216349] b)Nakashima Y, Mitsuhashi T, Matsuda Y, Senda M, Sato H, Yamazaki M, Uchiyama M, Senda T, Abe I, J. Am. Chem. Soc 2018, 140, 9743–9750. [PubMed: 29972643]

[14]. a)Matsuda Y, Awakawa T, Abe I, Tetrahedron 2013, 69, 8199–8204;b)Matsuda Y, Quan Z, Mitsuhashi T, Li C, Abe I, Org. Lett 2016, 18, 296–299. [PubMed: 26731665]

[15]. Matsuda Y, Bai T, Phippen CBW, Nødvig CS, Kjærbølling I, Vesth TC, Andersen MR, Mortensen UH, Gotfredsen CH, Abe I, Larsen TO, Nat. Commun 2018, 9, 2587. [PubMed: 29968715]

[16]. a)Matsuda Y, Iwabuchi T, Fujimoto T, Awakawa T, Nakashima Y, Mori T, Zhang H, Hayashi F, Abe I, J. Am. Chem. Soc 2016, 138, 12671–12677; [PubMed: 27602587] b)Zhang T, Wan J, Zhan Z, Bai J, Liu B, Hu Y, Acta Pharm. Sin. B 2018, 8, 478–487. [PubMed: 29881687]

[17]. a)Itoh T, Tokunaga K, Radhakrishnan EK, Fujii I, Abe I, Ebizuka Y, Kushiro T, ChemBioChem 2012, 13, 1132–1135; [PubMed: 22549923] b)Matsuda Y, Awakawa T, Itoh T, Wakimoto T, Kushiro T, Fujii I, Ebizuka Y, Abe I, ChemBioChem 2012, 13, 1738–1741; [PubMed: 22782788] c)Guo CJ, Knox BP, Chiang YM, Lo HC, Sanchez JF, Lee KH, Oakley BR, Bruno KS, Wang CCC, Org. Lett 2012, 14, 5684–5687; [PubMed: 23116177] d)Matsuda Y, Iwabuchi T, Wakimoto T, Awakawa T, Abe I, J. Am. Chem. Soc 2015, 137, 3393–3401. [PubMed: 25671343]

[18]. a)Araki Y, Awakawa T, Matsuzaki M, Cho R, Matsuda Y, Hoshino S, Shinohara Y, Yamamoto M, Kido Y, Inaoka DK, Nagamune K, Ito K, Abe I, Kita K, Proc. Natl. Acad. Sci. USA 2019, 116, 8269–8274; [PubMed: 30952781] b)Quan Z, Awakawa T, Wang D, Hu Y, Abe I, Org. Lett 2019, 21, 2330–2334. [PubMed: 30900461]

[19]. Tang MC, Cui X, He X, Ding Z, Zhu T, Tang Y, Li D, Org. Lett 2017, 19, 5376–5379. [PubMed: 28926261]

[20]. Qi C, Bao J, Wang J, Zhu H, Xue Y, Wang X, Li H, Sun W, Gao W, Lai Y, Chen JG, Zhang Y, Chem. Sci 2016, 7, 6563–6572. [PubMed: 28042460]

[21]. a)Inokuma Y, Yoshioka S, Ariyoshi J, Arai T, Hitora Y, Takada K, Matsunaga S, Rissanen K, Fujita M, Nature 2013, 495, 461–466; [PubMed: 23538828] b)Hoshino M, Khutia A, Xing H, Inokuma Y, Fujita M, IUCrJ 2016, 3, 139–151.

[22]. Yamazaki H, Nakayama W, Takahashi O, Kirikoshi R, Izumikawa Y, Iwasaki K, Toraiwa K, Ukai K, Rotinsulu H, Wewengkang DS, Sumilat DA, Mangindaan REP, Namikoshi M, Bioorg. Med. Chem. Lett 2015, 25, 3087–3090. [PubMed: 26115570]

[23]. a)Miehlich B, Savin A, Stoll H, Preuss H, Chem. Phys. Lett 1989, 157, 200–206;b)Lee C, Yang W, Parr GR, Phys. Rev. B 1988, 37, 785–789;c)Becke AD, J. Chem. Phys 1993, 98, 5648–5652;d)Grimme S, Ehrlich S, Goerigk L, J. Comput. Chem 2011, 32, 1456–1465; [PubMed: 21370243] e)Takano Y, Houk KN, Chem J. Theory Comput 2005, 1, 70–77.

[24]. We benchmarked our system using a variety of methods: CPCM(DCM)-B3LYP-D3(BJ)/6-31G(d,p)//B3LYP/6-31G(d,p), CPCM(MEOH)-B3LYP-D3(BJ)/6-31G(d,p)//B3LYP/6-31G-(d,p), mPW1PW91/6-31G(d,p)//B3LYP/6-31G(d,p) and CPCM-(MEOH)-mPW1PW91/6-31G(d,p)//B3LYP/6-31G(d,p). See SI for details. Matsuda SPT, Wilson WK, Xiong Q, Org. Biomol. Chem 2006, 4, 530–543. [PubMed: 16446812]

[25]. 9a is the conformer obtained from reverse **9a-TS** intrinsic reaction coordinate (IRC) analysis. **9a-TS** forward IRC product undergoes a conformational change to form **A** which is the reverse IRC product of **A-TS.** See SI for details.**9a-TS9a-TSAA-TS.** a)Gonzalez AC, Schlegel HB, J. Phys. Chem 1990, 94, 5523–5527;b)Fukui K, Acc. Chem. Res 1981, 14, 363–368;c)Maeda S, Harabuchi Y, Ono Y, Taketsugu T, Morokuma K, Int. J. Quantum Chem 2015, 115, 258–269.

[26]. Wang SC, Tantillo DJ, J. Org. Chem 2008, 73, 1516–1523. [PubMed: 18205383]

[27]. a)Tantillo DJ, J. Phys. Org. Chem 2008, 21, 561–570;b)Smentek L, Hess BA, J. Am. Chem. Soc 2010, 132, 17111–17117; [PubMed: 21080653] c)McCulley C, Geier MJ, Hudson BM, Gagne MR, Tantillo DJ, J. Am. Chem. Soc 2017, 139, 11158–11164. [PubMed: 28719198]

[28]. Abe I, Rohmer M, J. Chem. Soc. Perkin Trans 1 1994, 783–791.

[29]. a)Schulbach MC, Brennan PJ, Crick DC, J. Biol. Chem 2000, 275, 22876–22881; [PubMed: 10816587] b)Schulbach MC, Mahapatra S, Macchia M, Barontini S, Papi C, Minutolo F, Bertini S, Brennan PJ, Crick DC, J. Biol. Chem 2001, 276, 11624–11630. [PubMed: 11152452]

[30]. a)Nakashima Y, Mori T, Nakamura H, Awakawa T, Hoshino S, Senda M, Senda T, Abe I, Nat. Commun 2018, 9, 104–114; [PubMed: 29317628] b)Nakamura H, Matsuda Y, Abe I, Nat. Prod. Rep 2018, 35, 633–645. [PubMed: 29513321]

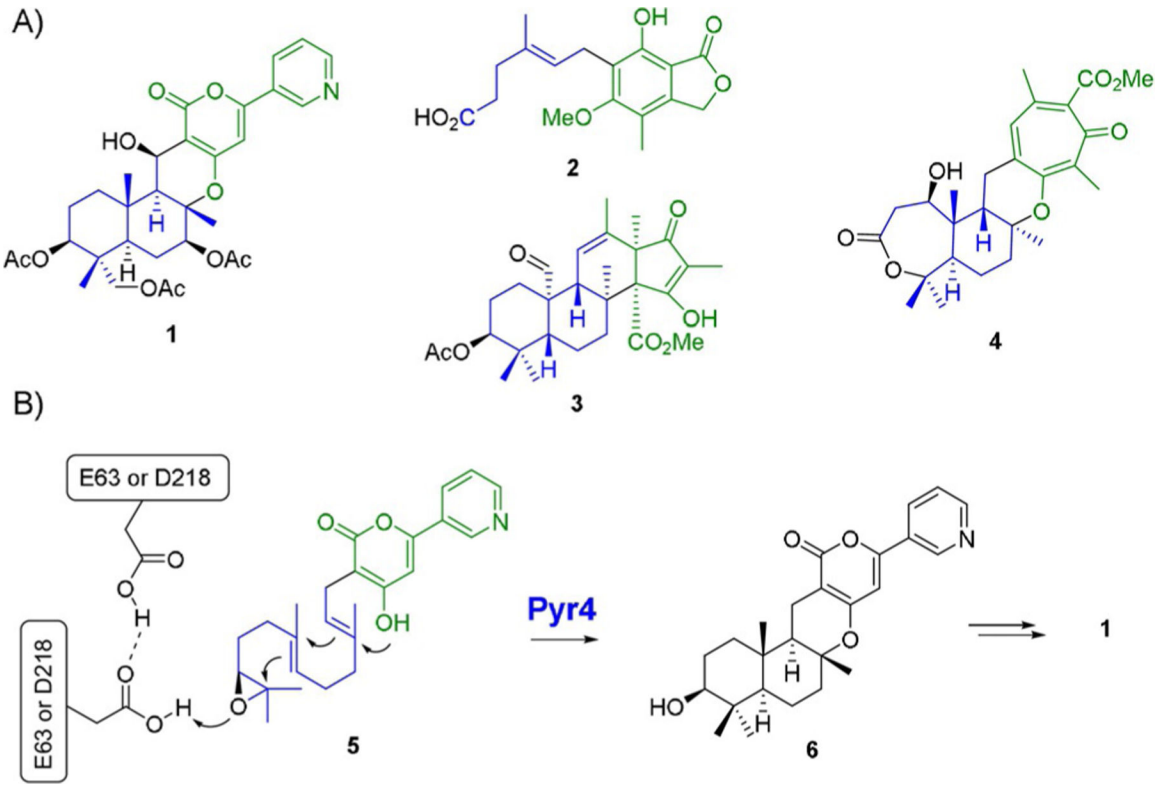

Figure 1.

A) Selected examples of fungal meroterpenoids. B) Proposed catalytic mechanism of meroterpenoid cyclases exemplified by Pyr4-mediated reaction of epoxyfarnesyl-HPPO (**5**) to deacetyl pyripyropene E (**6**). The polyketide portion is shown in green, terpenoid in blue.

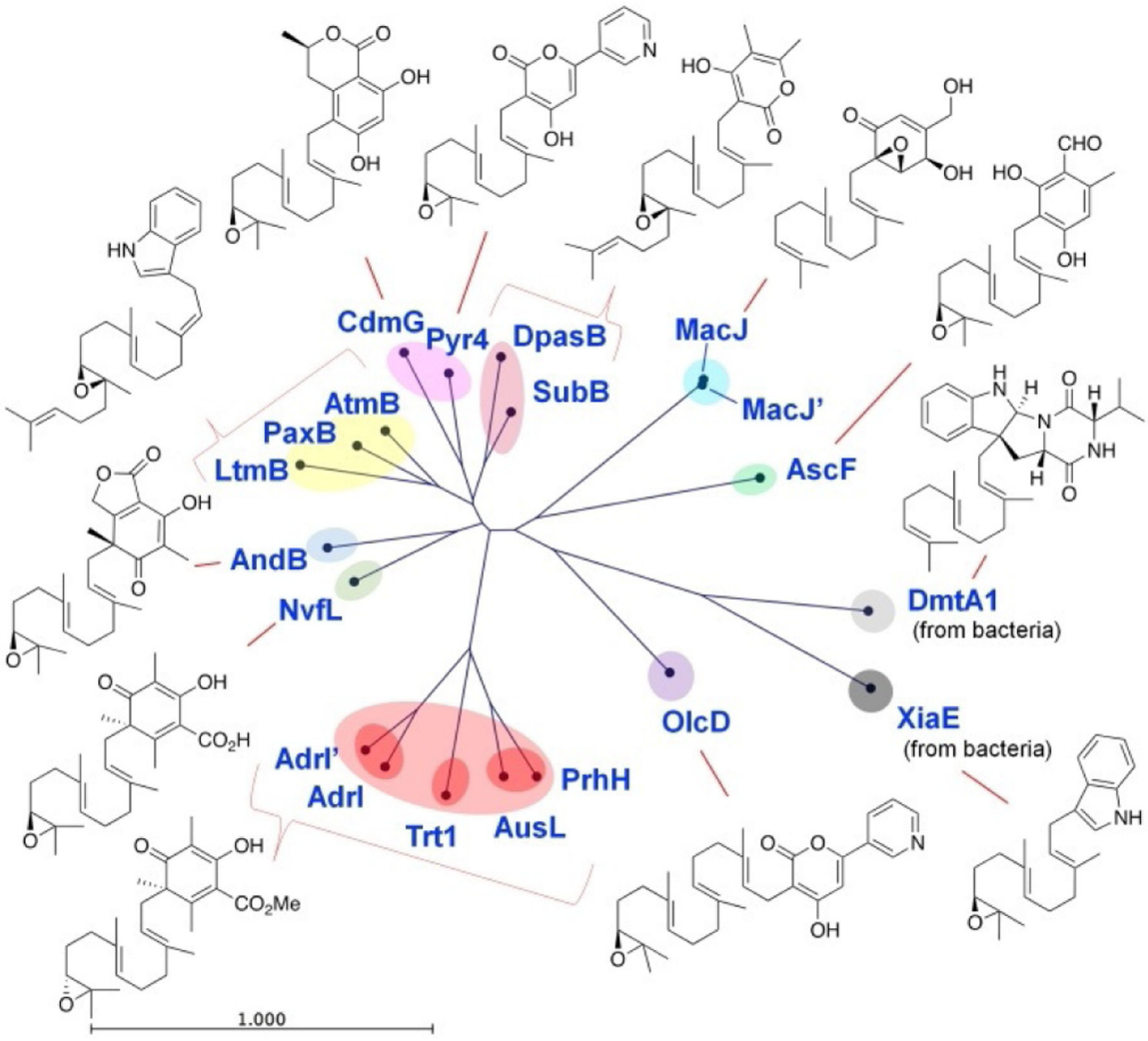

Figure 2.

Phylogenetic analysis of reported meroterpenoid cyclases and their respective native substrates.

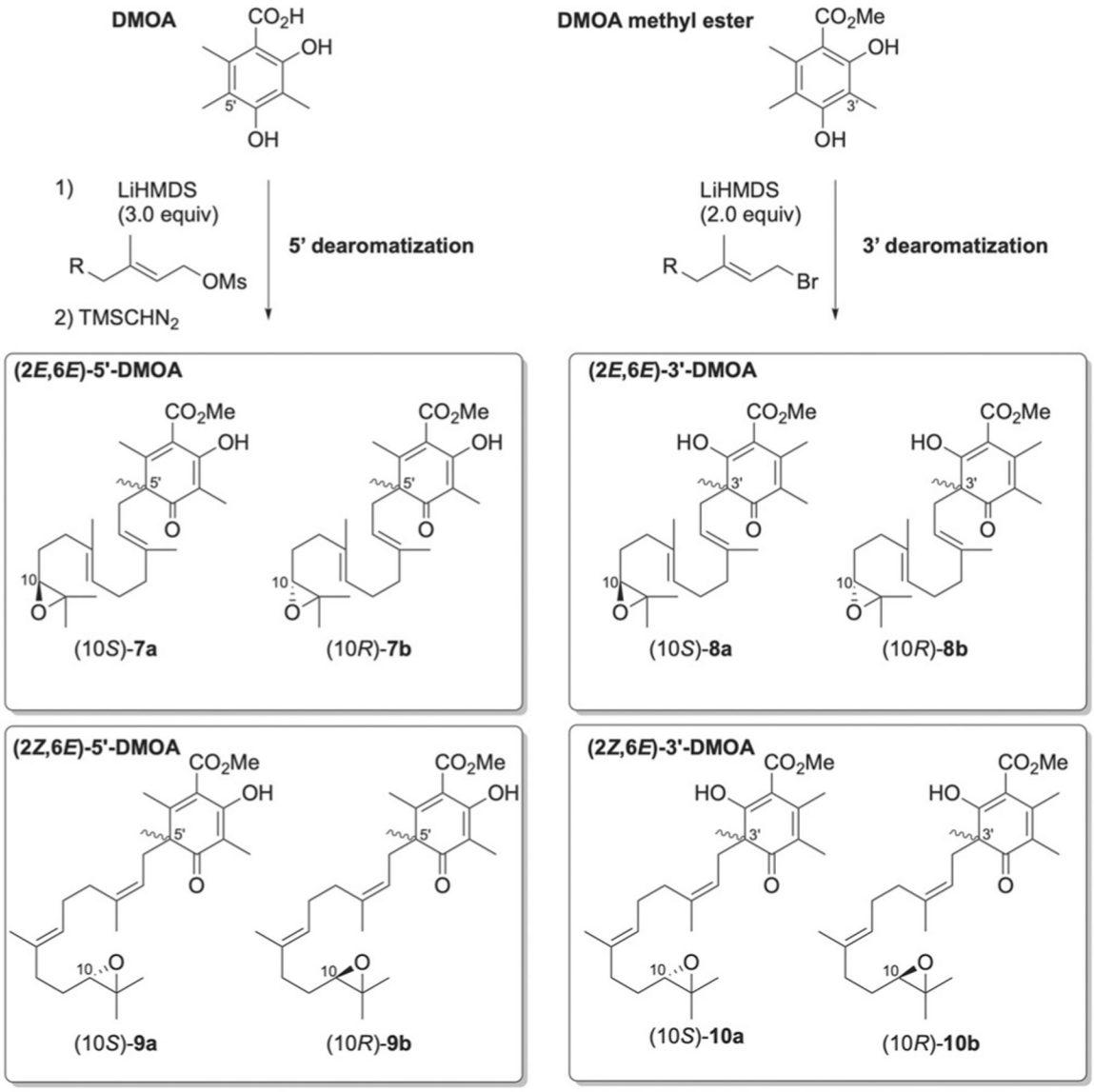

Figure 3.

Synthetic approach and structures of obtained and tested DMOA substrates (**7a/7b–10a/10b**).

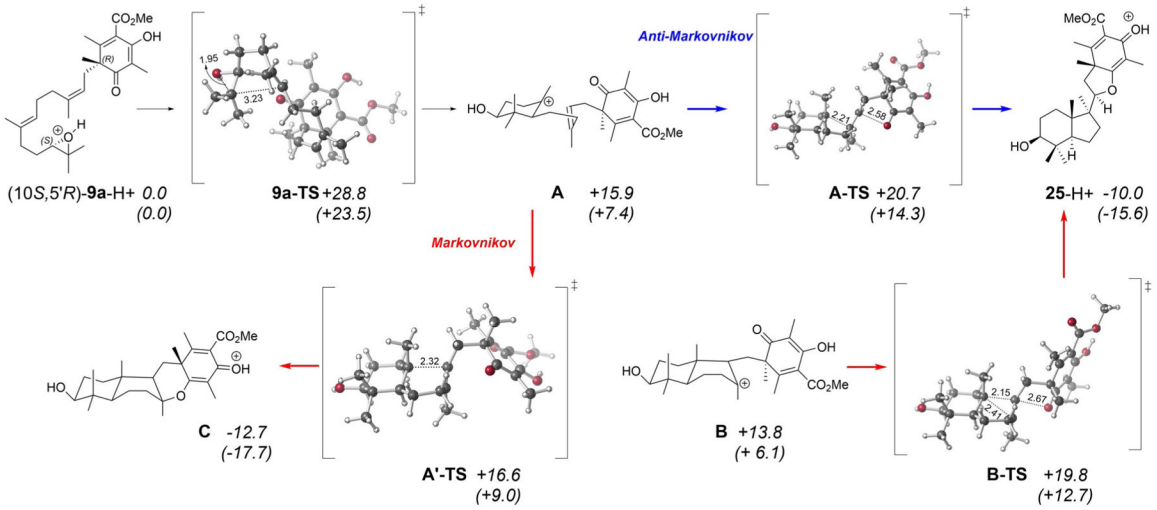

Figure 4.

DFT calculations for the cyclization mechanism of (10*S*,5′*R*)-**9a** towards **25** by AndB. Two conformers of **A** were located, one connected to **9a-TS** and another connected to **A-TS**, which differ in energy by 0–3 kcalmol^{-1}, depending on the level of theory; see SI for details. Computed (B3LYP-D3(BJ)/6-31G(d,p)//B3LYP/6-31G(d,p) in black (top), CPCM(H_2O)-B3LYP-D3(BJ)/6-31G(d,p)//B3LYP/6-31G(d,p) in parentheses (bottom)) relative free energies (kcalmol^{-1}, *italics*) for minima and transition state structures (TSSs) involved in formation of compound **25**. Bond distances are in Angstroms [Å].

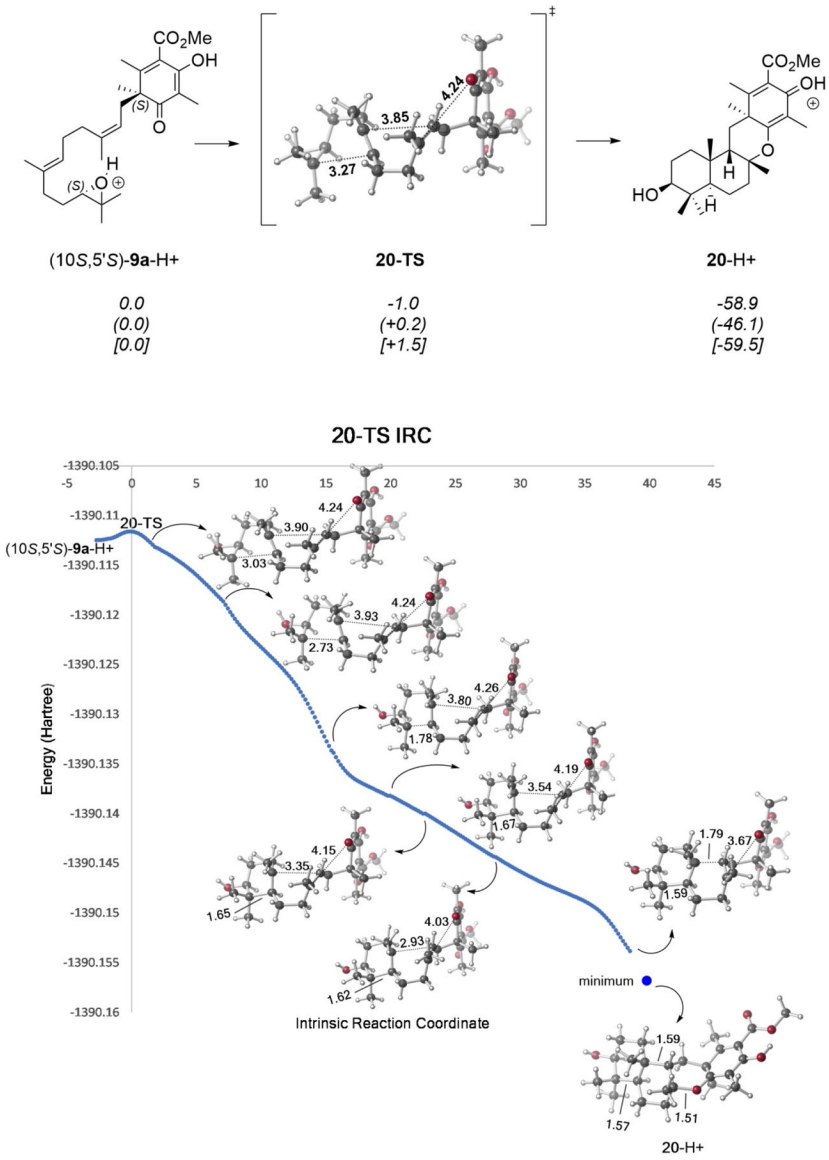

Figure 5.

DFT calculations for the cyclization mechanism for the formation of **20**. Computed (B3LYP-D3(BJ)/6-31G(d,p)//B3LYP/6-31G(d,p) (on top), CPCM(H2O)-B3LYP-D3(BJ)/6-31G(d,p)//B3LYP/6-31G(d,p) (in parentheses) and MPW1PW91/6-31G(d,p)//B3LYP/6-31G(d,p) [in brackets]) relative free energies (kcalmol^{-1}, italics) for minima and transition state structures (TSSs) and IRC traces for the respective TSSs. Bond distances are in Angstroms [Å].

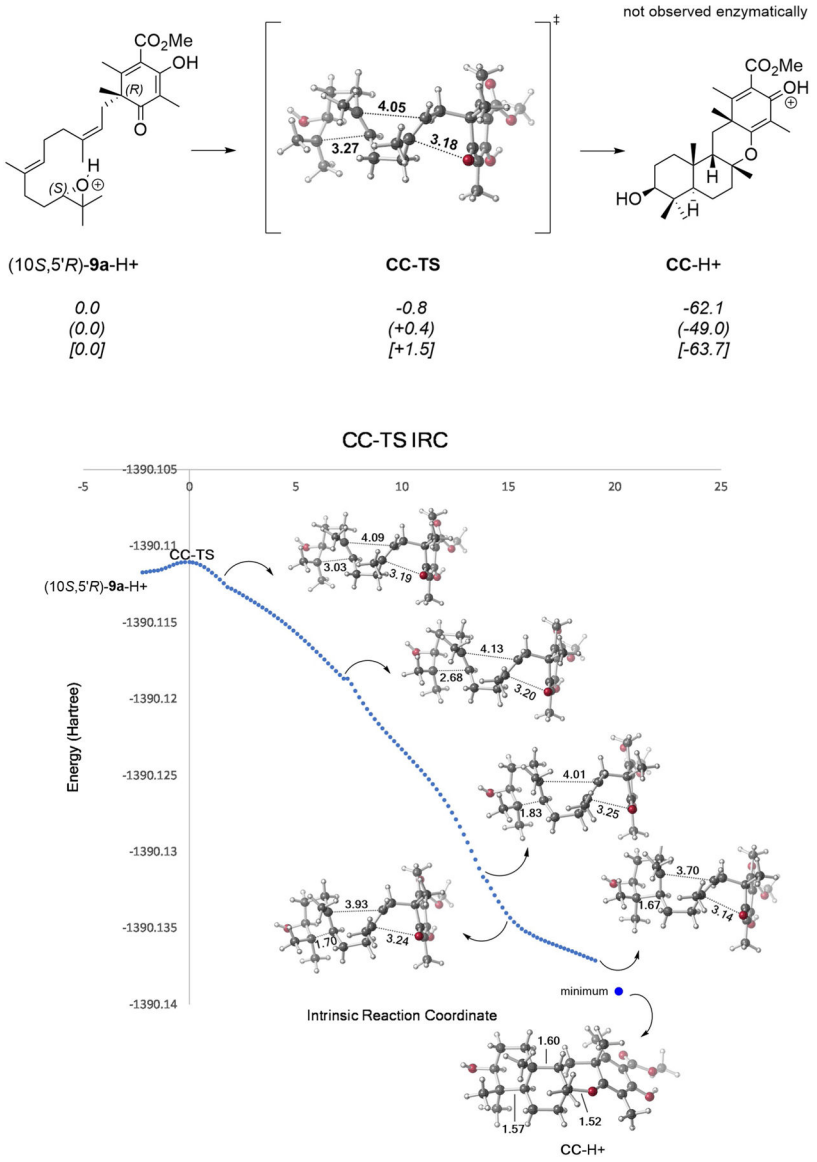

Figure 6.

DFT calculations for the cyclization mechanism for the formation of **CC**. Computed (B3LYP-D3(BJ)/6-31G(d,p)//B3LYP/6-31G(d,p) (on top), CPCM(H2O)-B3LYP-D3(BJ)/6-31G(d,p)//B3LYP/6-31G(d,p) (in parentheses) and MPW1PW91/6-31G(d,p)//B3LYP/6-31G(d,p) [in brackets]) relative free energies (kcalmol^{-1}, italics) for minima and transition state structures (TSSs) and IRC traces for the respective TSSs. Bond distances are in Angstroms [Å].

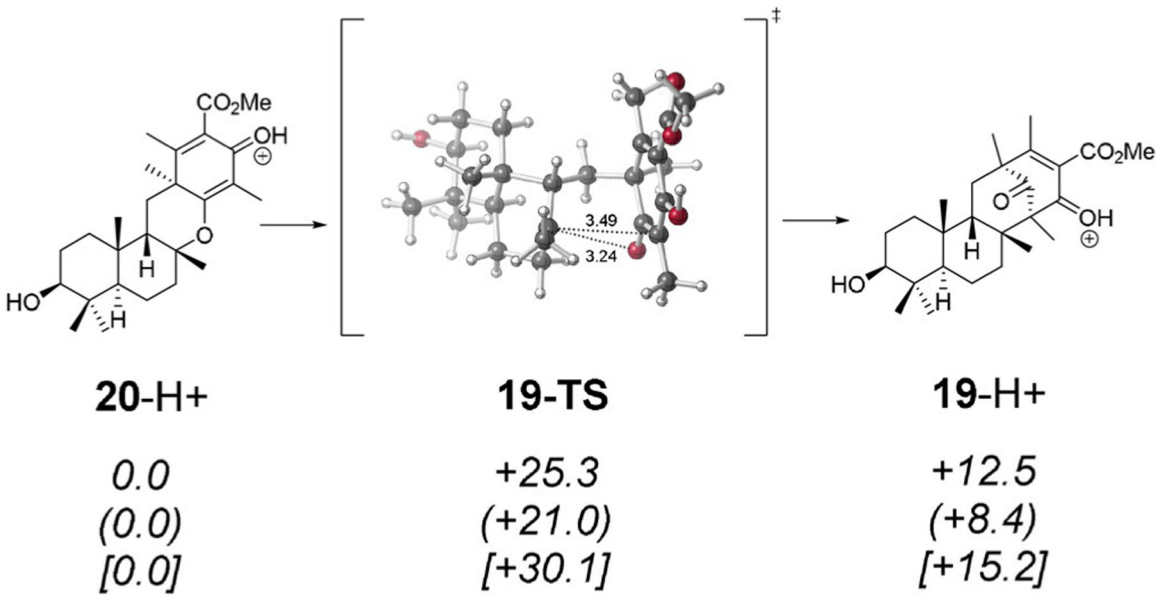

Figure 7.

DFT calculations for the interconversion of **20**-H^+ to **19**-H^+. Computed (B3LYP-D3(BJ)/6-31G(d,p)//B3LYP/6-31G(d,p) (on top), CPCM(H_2O)-B3LYP-D3(BJ)/6-31G(d,p)//B3LYP/6-31G(d,p) (in parentheses) and MPW1PW91/6-31G(d,p)//B3LYP/6-31G(d,p) [in brackets]) relative free energies (kcalmol^{-1}, *italics*) for minima and transition state structures (TSSs). Bond distances are in Angstroms [Å].

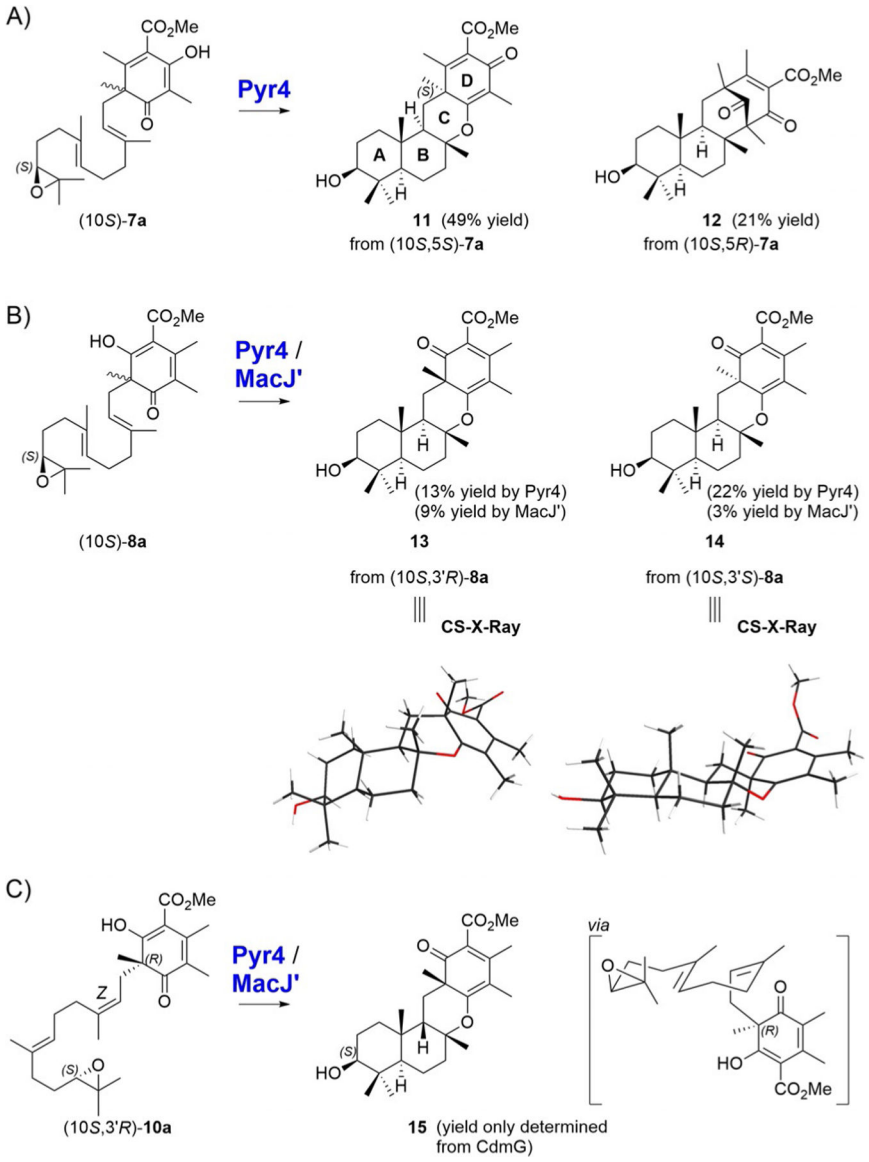

Scheme 1.

Structures of isolated meroterpenoids obtained from Pyr4- and MacJ′-mediated reactions with A) (10*S*)-**7a**; B) (10*S*)-**8a**; C) (10*S*,3′*R*)-**10a**.

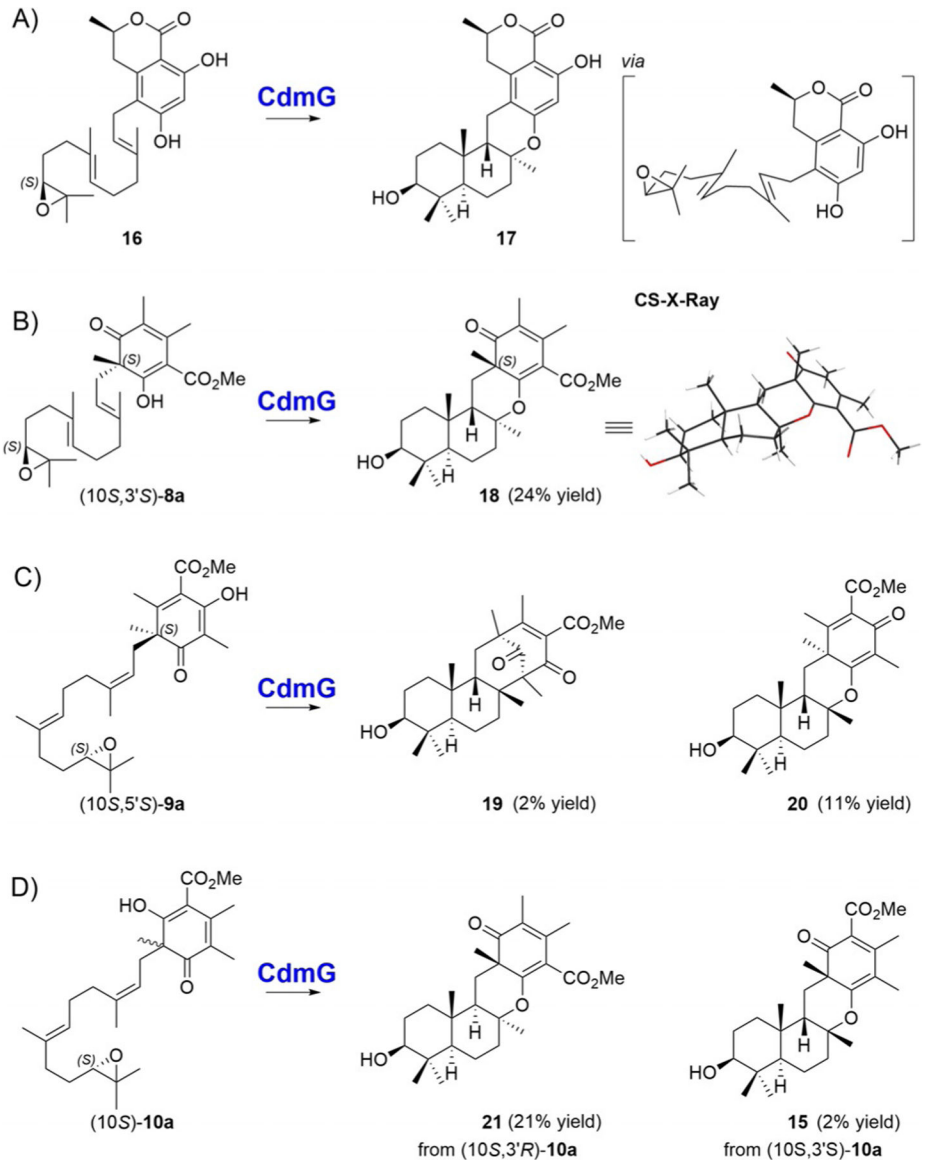

Scheme 2.

A) Natural Reaction of CdmG and isolated meroterpenoids obtained from CdmG-mediated reactions with B) (10*S*,3′*S*)-**8a**; C) (10*S*,5′*S*)-**9a**; D) (10*S*)-**10a**.

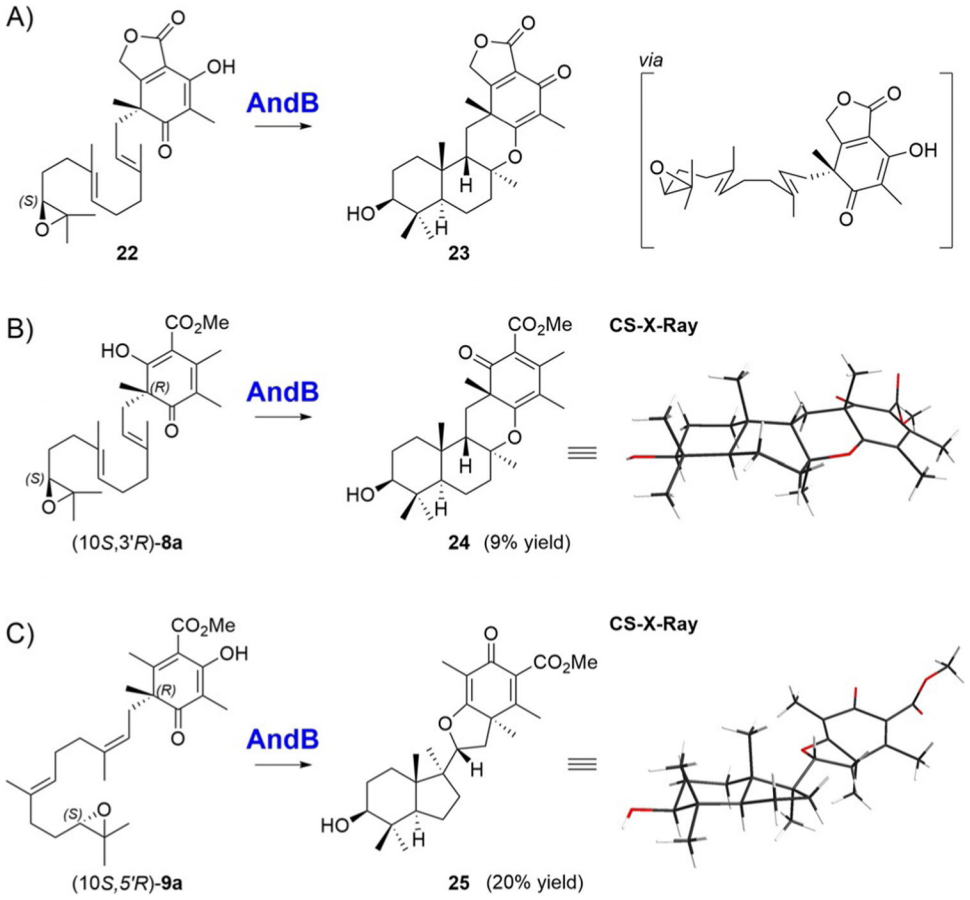

Scheme 3.

A) Natural reaction of AndB and structures of isolated meroterpenoids obtained from AndB-mediated reactions with B) (10*S*,3′*R*)-**8a**; C) (10*S*,5′*R*)-**9a**.

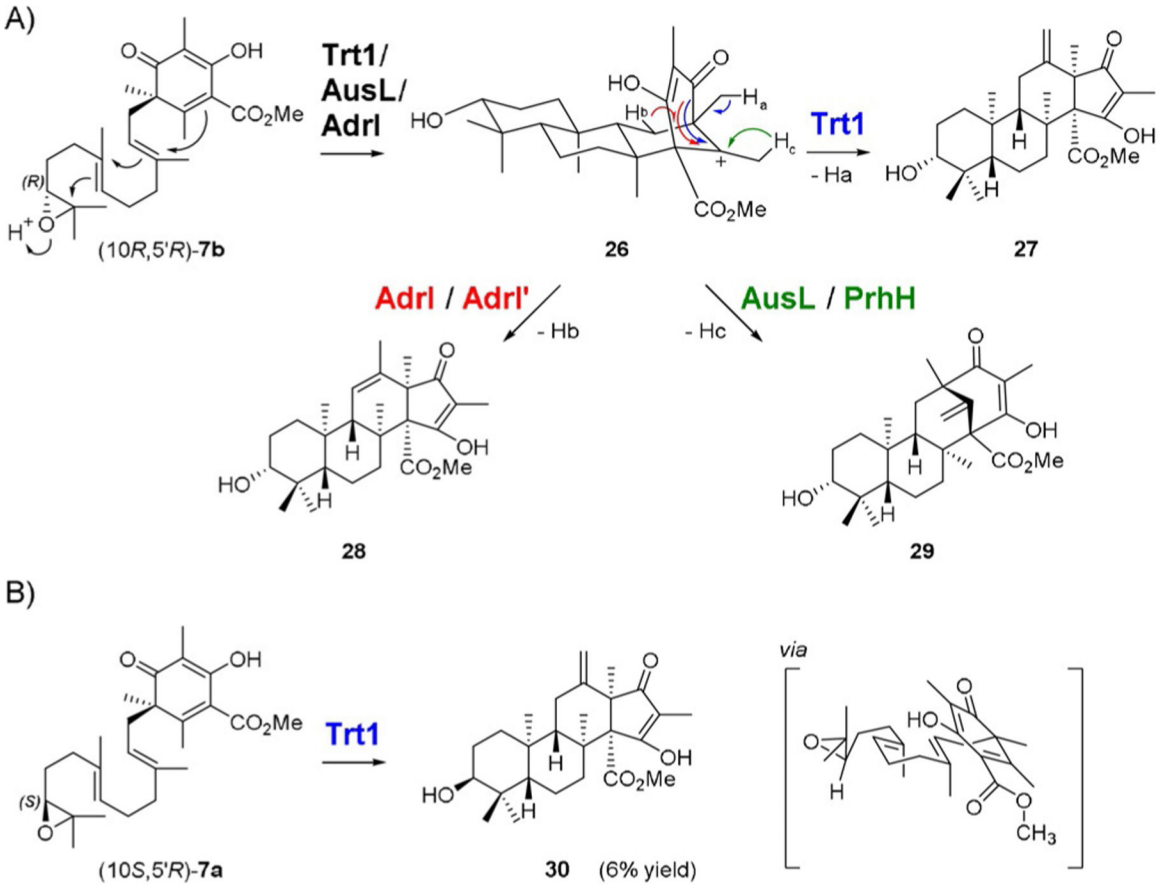

Scheme 4.

A) Natural reaction of Trt1, AdrI/AdrI′ and AusL/PrhH. B) Isolated meroterpenoids obtained from Trt1-mediated reactions with (10*S*,5′*R*)-**7a**.

Table 1:

Overview on productive enzyme substrate combinations.

	(2*E*,6*E*)-5′-DMOA	**(2*E*,6*E*)-3′-DMOA**	**(2*Z*,6*E*)-5′-DMOA**	**(2*Z*,6*E*)-3′-DMOA**
Pyr4	(10*S*)-**7a**	(10*S*)-**8a**	–	(10*S*)-**10a**
MacJ′	(10*S*)-**7a**	(10*S*)-**8a**	–	(10*S*)-**10a**
CdmG	(10S)-**7a**	(10*S*)-**8a**	(10*S*)-**9a**	(10*S*)-**10a**
AndB	(10*S*)-**7a**	(10*S*)-**8a**	(10*S*)-**9a**	–
Trt1	(10*S*)-**7a** (10*R*)-**7b**[a]	–	(10*R*)-**9b**	–
AdrI′	(10*S*)-**7a** (10*R*)-**7b**[a]	–	(10*R*)-**9b**	–
PrhH	(10*R*)-**7b**[a]	–	–	–
NvfL	–	–	–	–
AscF	–	–	–	(10*S*)-**10a**

[a]Native enzyme substrate combination.